Available online at www.sciencedirect.com
ScienceDirect
Materials Chemistry and Physics 103 (2007) 35–40
MATERIALS CHEMISTRY AND PHYSICS
www.elsevier.com/locate/matchemphys

Effect of backbone on the biaxial retardation of polyimide films in uniaxial stretch

Jinn-Shing King [a], Wha-Tzong Whang [a,*], Wen-Chin Lee [b], Li-Ming Chang [b]

[a] *Department of Materials Science and Engineering, National Chiao Tung University, Hsinchu 300, Taiwan, ROC*
[b] *Material and Chemical Research Laboratories, Industrial Technology Research Institute, Building 77, No. 195, Section 4, Chung Hsing Road, Chutung, Hsinchu 310, Taiwan, ROC*

Received 16 June 2006; received in revised form 23 November 2006; accepted 13 December 2006

Abstract

A biaxial-retardation film prepared from the uniaxial-stretched polyimide (PI) film was developed for compensating the viewing angle of liquid-crystal displays. Good uniformity of in-plane birefringence in well-stretched PI films was observed visually with two crossed polarizers. The prism coupling method was used to measure the n_x, n_y, n_z, and thickness of the stretched PI films. The birefringence variations of $n_x - n_y$ (difference of refractive indices between x- and y-axes) and $n_x - n_z$ during the stretching process were highly affected by PI structure. The polarizability tensors and intrinsic birefringences of the PI repeat units were estimated by Gaussian 98W. It was found that the stretch-induced birefringence is more related to the average polarizability per volume at the low elongation period.

Keywords: Optical materials; Polyimide; Computer modelling and simulation; Birefringence

1. Introduction

Polymer films with large anisotropic optical properties are not favored in communication media application such as polymer waveguides [1,2]. On the other hand, large birefringent polymer films have important application in optical films for liquid crystal display (LCD) [3–6]. Therefore, methods are needed to adjust the optical anisotropies between minimum and maximum values for optimization in different applications. The stretch or draw method is now a common used way in industry to induce the birefringence of optical films.

Optical anisotropies of polymer films are mostly related to the chemical structures and fabrication processes. Some polymers with rigid structure show high birefringence after casting film on substrates. Aromatic polyimides (PIs) were found to be used as uniaxial negative birefringent compensators (negative C plate) for twisted nematic (TN) LCDs by Dr. Harris since 1996 [3,4]. In this case, birefringence of polyimide films could be adjusted by varying chemical structures through the copolymerization. However, negative C plate can only compensate the light leakage from the LC layer. Light leakage from the crossed polarizer, in the off-axis, is a serious problem in high-quality LCDs that require a wide-angle view and high contrast ratio in all azimuthal directions. A conventional method to compensate both the light leakage from the LC layer and crossed polarizer is using a combination of an A- and C-plate [5,6]. Another alternative is to use biaxial retardation films [7]. The A-plate or biaxial retardation film is usually fabricated through stretching or drawing polymer films [8]. Due to the low birefringence, the commercial compensation films need high thickness (>80 μm). Moreover, two sheets are usually required to have enough compensating performance.

To simultaneously overcome the high thickness and high cost problems of the wide-viewing-angle polarizer in the high competitive LCD industry, we suggested a biaxial retardation film of high retardation value by uniaxially stretching a thin polyimide film in an earlier publication [9]. We found that the birefringence generated by a uniaxial stretch was greatly affected by the structure of PI backbone. However, detailed mechanisms governing how the PI structure affects the induced birefringence have not been fully understood. Recently, new studies on intrinsic birefringence for the PIs having various aromatic structures were reported [10–12]. We think the intrinsic birefringence may play a key role in the structural effects on the stretched-induced birefringence. Moreover, little is known about the influence of main

* Corresponding author.
E-mail address: wtwhang@mail.nctu.edu.tw (W.-T. Whang).

0254-0584/$ – see front matter © 2006 Elsevier B.V. All rights reserved.
doi:10.1016/j.matchemphys.2006.12.005

chain structure on the induced birefringence when the elongation is low.

This paper described the results of the studies on stretch-induced birefringence using different main chain structures while keeping the same stretch conditions. We have prepared two low-T_g polyimides based on 4,4′-(4,4′-isopropylidenediphenyl-1,1′-diyldioxy) dianiline (BAPP) which has soft and bended structure. Two dianhydrides of aromatic and aliphatic structures were used to modify the main chain structures of PIs. The PI films were obtained and successfully stretched at 260 °C. Their applications as LCD retardation films were evaluated, and the correlation between PI structures and stretch-induced birefringence was discussed.

2. Experimental

2.1. Materials

In our experiments, 4,4′-(hexafluoroisopropylidene)diphthalic anhydride (6FDA) was purchased from Aldrich. 3,4-Dicarboxy-1,2,3,4-tetrahydro-1-naphthalenesuccinic acid dianhydride (D2192) was obtained from TCI. 4,4′-(4,4′-Isopropylidenediphenyl-1,1′-diyldioxy) dianiline (BAPP) was obtained from Chriskev. 6FDA was purified by sublimation under reduced pressure before use. D2192 and BAPP were used as received. *N*-Methyl-2-pyrrolidone (NMP) was dried via the benzene azeotrope. As the precursors of PI, poly(amic acid) (PAA) solutions were prepared by the polycondensation reaction of one dianhydride and the BAPP diamine in NMP. The respective dianhydride was added to the BAPP solution and mechanically stirred at 25 °C for 48 h under N_2 purge. The inherent viscosities of the obtained PAA solutions were measured using Ubbelohde viscometers at a concentration of 0.5 g dl^{-1} at 25 °C. The measured PAA viscosities of D2192-BAPP (D-B) and 6FDA-BAPP (6F-B) were 0.67 and 0.63 dl g^{-1}, respectively. PAA films were prepared by soft baking of PAA solutions on poly(ethylene terephthate) (PET) films at 70 °C for 1 h. The PAA films were removed from the PET films, fixed between two steel frames, and then step heated to 300 °C in N_2 oven. The resulting 20 micron-films of D2192-BAPP and 6FDA-BAPP were colorless and slightly yellow, respectively. The D-B film and 6F-B film exhibited glass transitions at 250 and 254 °C, respectively under the TMA (Thermal mechanical analysis, Q400 by TA Instrument) method.

2.2. Stretch of PI films

To stretch the polyimide film, we used the dynamic mechanical analyzer (DMA 2980 by TA Instrument). Stress relaxation method set-up in the software of DMA 2980 was used to perform the stretch process. The five controlled factors were preload force (N), strain (%), isothermal temperature (°C), soak time (min), and relaxation time (min). Preload force is a key factor to control the extending ratio when other factors are suitable. The isothermal temperature and soak time were set to be 260 °C and 5 min, respectively, according to a series of pretests with several D-B films.

2.3. Measurement of optical property

A UV–vis spectrometer (Lambda 900 by Perkin-Elmer) with an integrating sphere (PELA-1020 by Labsphere Inc.) was used to evaluate the Haze and transparency of the prepared PI films. The measurement of Haze followed the ASTM 1003-92 standard method.

To analyze the birefringence change in stretched PI films, the prism coupling method (SPA-4000 by SAIRON Technology) was used to measure the n_x, n_y, n_z, and thickness of the stretched PI films. The principle and instrumental set-up has been described elsewhere in detail [13,14]. The two in-plane refractive indices (RI), n_x and n_y, and the film thickness were obtained from two measurements with s-light in parallel and perpendicular to the sample stretch direction. From corresponding measurements using p-light, the refractive index normal to the film plane (n_z) was obtained. Due to the necking problem in some samples under high preload force, three points of each sample were measured at a wavelength of 632.8 nm. A wafer was used as a substrate to carry the samples which were pressed against the prism uniformly. For accurate measurements, the thickness of PI films should not be larger than 20 μm.

2.4. Calculation of polarizability tensor

The Gaussian 98W program package (version 5.4) was used for Hartree–Fock (HF) and the density functional theory (DFT) calculations for PI repeat units of D2192-BAPP and 6FDA-BAPP. The B3LYP hybrid functional was employed in the DFT calculations. The semi-empirical method (AM1) of Hartree–Fock theory (HyperChem Pro 6, version 6.03) was used to optimize the structures of PI repeat units. The STO-3G and 6-31G of B3LYP were used to calculate the molecular polarizability and volume of the optimized PI structures.

3. Results and discussion

3.1. Stretch conditions of PI films

The stretch of PI films was performed by DMA 2980. The preload force was designed to be a key factor for controlling the extending ratio. For this purpose, we did some pretests for seeking the suitable stretch conditions with the D-B films. The test results are summarized as follows. First, under long relaxation times, all stretched samples would extend to maximum elongation (limited by the chamber size of DMA 2980) even at the smallest preload force. Thus, we set a short relaxation time of 0.01, in order to examine the effect of the preload force. Second, as the high strain exacerbates the necking problem of stretched samples the strain factor was limited to no more than 0.05, usually 0.01.

The stretched samples of PI films are shown in Fig. 1. With the open-chamber system of our DMA 2980, even nitrogen purge could not prevent yellowing (due to oxidation) of most D-B films during the stretching period at 260 °C, which is higher than the T_g of the PI film (see the three samples on the right in Fig. 1). However, the stretched D-B films under large preload force (such as over 0.2 N) and without nitrogen purge were colorless. Perhaps the large preload force required a shorter time to reach maximum elongation at the over-T_g temperature and did not allow enough time for the film to yellow (see the two samples on the left in Fig. 1). The necking phenomenon of D-B films after stretching under large preload forces was significant because we did not have proper clamping apparatus. However, such necking phenomenon should not occur at biaxial-stretch production lines in industry.

3.2. Optical properties of haze and transparency

The calculated Hazes of D-B film and 6F-B film are smaller than 0.1 and 0.16, respectively, at the scanned wavelength from 780 to 380 nm. Fig. 2 shows the visible spectrum of PI films that measured with the same integrating sphere. Both PI films showed high transparency close to 89% at 550 nm. The 6F-B film showed lower transparency than D-B film at wavelength lower than 480 nm. The D-B film showed excellent colorless quality as compared with other PI films without fluorine atoms [15].

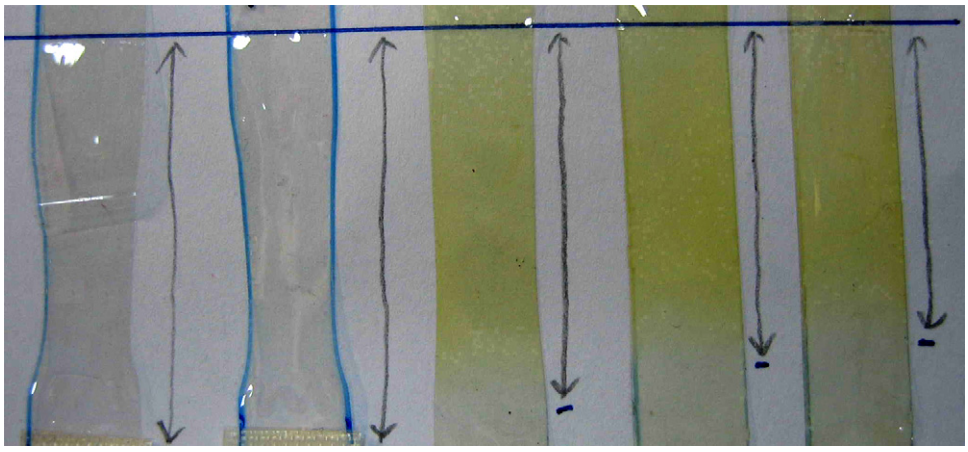

Fig. 1. A photo of five stretched PI films that were composed of the D2192-BAPP. The left two samples were stretched under large preload force.

3.3. Birefringence and elongation

The birefringence of the stretched sample was evaluated by measuring the RIs which are parallel and perpendicular to the stretch direction applied on PI films. The sample thickness is a critical issue to get a suitable RI data in different modes of SPA-4000. Fig. 3 shows the measured results of PI samples with different thickness. With a suitable film thickness (a), high quality data of the refractive index and the thickness can be observed in the low standard deviation under the single layer mode. With a thick film of thickness above 20 μm (b), the refractive index can only be measured as the bulk sample without the thickness data. The measured RI data can only be compared when they were all come from the same mode.

The n_x, n_y, and n_z of the stretched PI films with controlled elongation ratios were showed in Fig. 4. Fig. 4 shows the variations of n_x, n_y, and n_z induced from the elongation change of D-B films and 6F-B films. To analyze the correlation between the birefringence variations and elongation degrees of PI films, we took stretched D-B films as the example. Birefringence $(n_x - n_y)$ of the stretched D-B film was calculated from the measured RI and shown in Fig. 5. The preload force was the key factor to control the stretch condition. The left part in Fig. 5 shows the correlation between preload force and the birefringence of stretched samples. The preload force was varied from 0.01 to 0.3 N while the birefringence (in average, right part in Fig. 5) induced increased from 0.0004 to 0.0176. The non-uniformity of birefringence induced by necking phenomenon was observed in the sample with high preload force of 0.3. Usually, point 2 was close to the neck position of sample, which was near the pulling side. The stretch ratio of D-B film reached a limit (limited by chamber size of DMA 2980) when the preload force exceeded 0.2 N at 260 °C. The excessive preload force of 0.3 N generated a necking area in the PI film. Consequently a higher birefringence near point 2 was induced, which increased the average value of birefringence of this sample. In conclusion, adjustment of the stretching force is important for generating uniform birefringence in PI films.

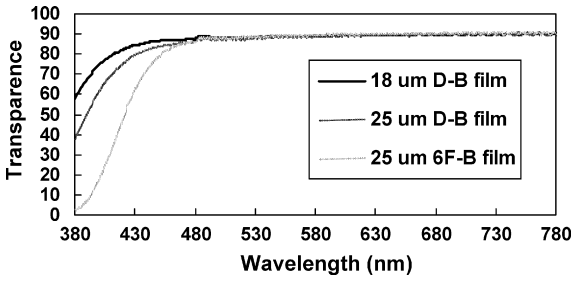

Fig. 2. The visible spectrum of PI films that measured with an integrating sphere.

3.4. Relaxation of stretched PI film

The relaxation behaviors of two stretched PI films with the same elongation were observed by TMA method with a force of 0.05 N. Two plots of measured results were overlaid in Fig. 6. The stretched 6F-B film showed more intense shrinkage than the D-B film when the temperature was higher than their T_gs. The different relaxation behaviors may be attributed to their difference in the structures of aromatic and aliphatic backbones. The correlation between the relaxation behavior and PI structure will be discussed further in a later section.

3.5. Structure effect

In the final part of this study, we discuss the effect of PI structure on the induced birefringence with a stretch. Fig. 4 shows the variations of n_x, n_y and n_z, which were induced by the elongation change of D-B films and 6F-B films. The non-stretch 6F-B films show lower RI than D-B films. Because of the soft and bended structure of aliphatic dianhydride and BAPP diamine, the out-of-plane birefringence (TE − TM or $n_x - n_z$) of D-B films is very low, down to 0.0007. With an increase in elongation ratio, the in-plane birefringence $(n_x - n_y)$ increased sharply after a slow rise at beginning. It is interesting to note that the out-of-plane birefringence also increased significantly with the increase of elongation ratio. The fact that n_z and n_y have the same trend of RI variation is not surprising as this had been reported in earlier publications [16]. But we found the degrees of RI variation in y- and z-axes to be almost the same, which may be attributed to the initial soft and bended structure

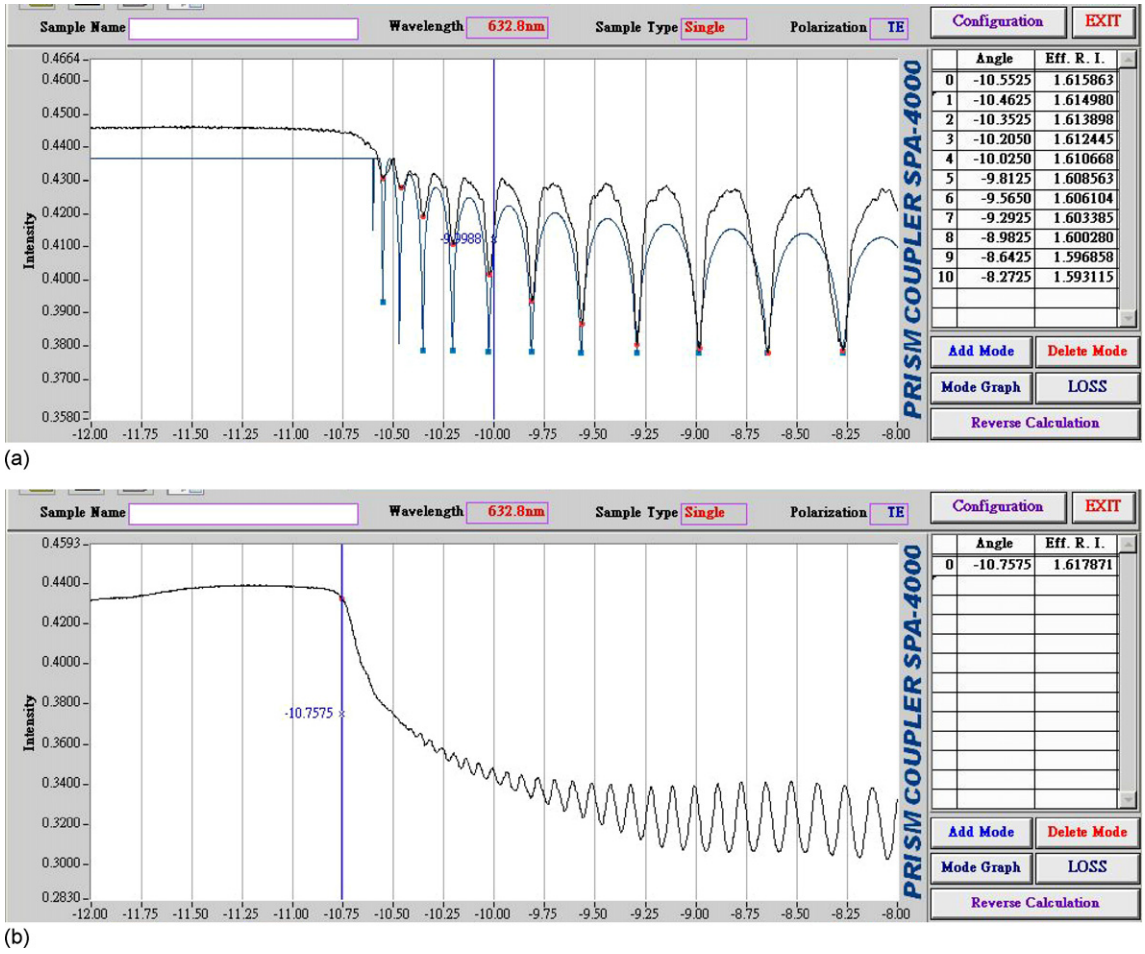

Fig. 3. The spectra of the prism coupler method under the single layer mode (a) and bulk sample mode (b).

of D2192-BAPP. The rearrangement of polymer chains during stretch period showed the same influence on in-plane ($n_x - n_y$) and out-of-plane ($n_x - n_z$) anisotropies of D-B films.

The RI variation of 6F-B films in Fig. 4 shows more gradual change with the increase of elongation ratio, when compared with that of D-B films. At the same elongation ratio (=0.2), 6F-B film exhibits more than three times larger birefringence than D-B film does. Although the 6FDA-BAPP has a fully aromatic structure, the bended structure and soft linkage group give the 6F-B film low out-of-plane (TE − TM or $n_x - n_z$) birefringence (=0.0012). However, the larger dipole moment of 6F-B polymer chains induces higher degree of chain–chain interaction [16]

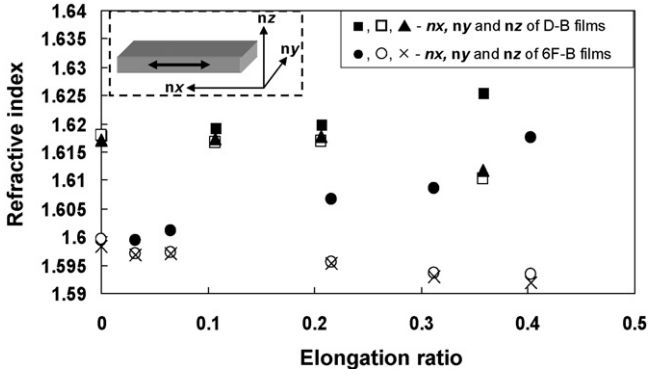

Fig. 4. Refractive indices of each axis, n*x*, n*y* and n*z*, in D-B films and 6F-B films at different elongation ratios. The arrow in the illustration corresponds to the stretch direction applied on the PI films.

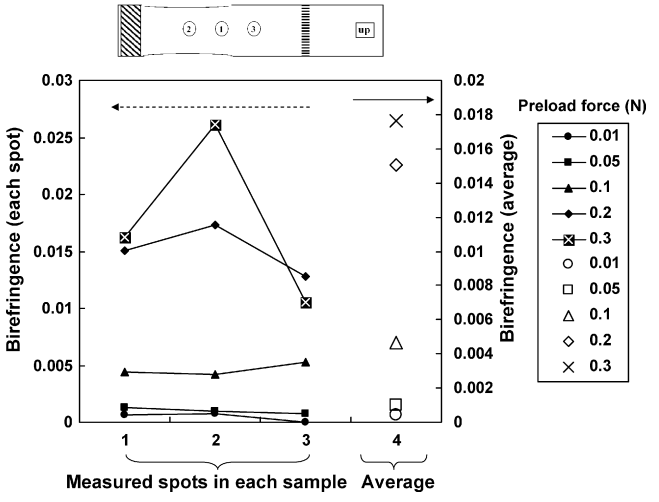

Fig. 5. The birefringence of stretched D-B films at different preload forces. Left *y*-axis shows the birefringence data that correspond to their measuring sites in each sample. Right *y*-axis shows the average birefringence of each stretched D-B film.

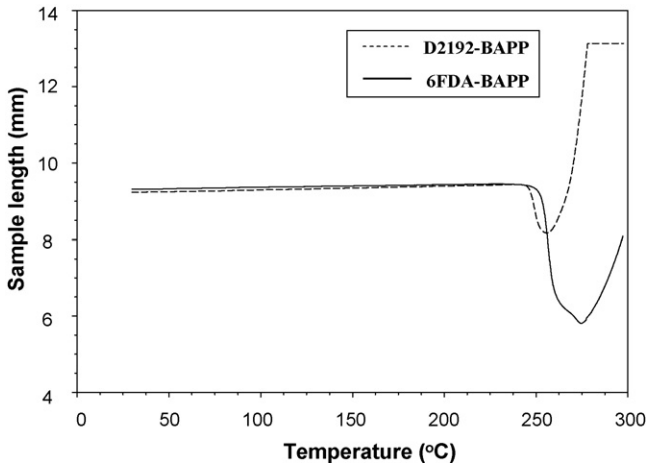

Fig. 6. The TMA spectrum of the stretched D-B film and 6F-B film.

$$n_i=[(((n_{av}{}^2+2)4\pi \mathbf{K_p}\alpha_i)/(3V_{vdw}))+1]^{1/2}$$

$$K_p= [3(n_{av}{}^2-1)/4\pi(n_{av}{}^2+2)]/(\alpha_{av}/V_{vdw})$$

$$n_{av}=[(2n_{TE}{}^2+ n_{TM}{}^2)/3]^{1/2}$$

$$\Delta n^0=n_{//}{}^0-n_{\perp}{}^0$$

$$\alpha_{av}=(\alpha_{XX}+\alpha_{YY}+\alpha_{ZZ})/3$$

$$\Delta\alpha=\alpha_{ZZ} - (\alpha_{XX}+\alpha_{YY})/2$$

Fig. 7. The equations used for calculating the packing coefficient and intrinsic birefringence. The n_i stands for $n_{||}^0$ or $n_{\perp}^0$ while α_i stands for α_{ZZ} or the average of α_{XX} and α_{YY}.

during the stretch process. Hence, 6F-B films exhibit larger birefringence at the same elongation ratio when compared with D-B films. The above inference was made according to the viewpoint of large dipole moment that belongs to the aromatic structure. More experimental evidence is necessary to support this inference.

3.6. Calculation of intrinsic birefringence

Further studies on the effect of PI structure were conducted with suitable simulation methods [12] to clarify the influence of molecular polarizability on the induced birefringence. We think the dipole-dipole interaction could be a major force in chain–chain interaction. Besides, calculating the intrinsic birefringence of polyimide structure may give us more information to uncover the mystery of stretching-induced birefringence. According to Dr. Ando's method [12], intrinsic birefringence of polyimides can be estimated using refractive indices and molecular polarizabilities. The refractive indices were measured by SPA-4000 in this study. The calculation of polarizability tensor was performed with Gaussian 98W program package (version 5.4). Due to the large molecular size of BAPP monomer, both repeat units of D-B and 6F-B PI have primitive Gaussians over 1500 using B3LYP/6-31G(d) level of theory. The calculations of our PI repeat units were dead-linked before finish. Although the 6-31G(d) level was suggested for optimizing the molecular geometry of the PI models, we use the optimized PI structure from the semi-empirical method (AM1) of HyperChem Pro 6 to calculate the polarizability tensor and molecular volume. The semi-empirical method of Hartree–Fock theory may give acceptable results of optimization for large organic molecules. We used B3LYP/STO 3G, B3LYP/6-31G, and B3LYP/6-31+G(d) to calculate the polarizability and molecular volume of the optimized PI structure. The primitive Gaussians of B3LYP/6-31+G(d) method which suggested in literature [12] were still too high for our PI repeat units to finish the calculation. And thus the following analysis was based on the results from the lower level of calculations. Table 1 shows the calculated values of molecular volumes, and each principal component of polarizability tensor (α_{XX}, α_{YY}, and α_{ZZ}) from Gaussian 98W. Other listed values of average polarizability per volume ($\alpha_{av}/V_{molecule}$), polarizability anisotropy per volume ($\Delta\alpha/V_{molecule}$) and packing coefficient (K_p) of PIs were calculated based on the equations listed in Fig. 7. These equations were all conducted or represented from the earlier work in the literature [12]. For simplifying the simulation work, we used molecular volumes ($V_{molecule}$) instead to replace the van der Waals volumes (V_{vdw}) showed in Fig. 7. Table 2 shows the in-plane (n_{TE}) and out-of-plane (n_{TM}) refractive indices of PI films at 632.8 μm. Other listed values of average refractive indices (n_{av}), in-plane/out-of-plane birefringence (Δn) and intrinsic birefringence (Δn^0) of

Table 1
Results of Gaussian 98W calculations and estimated packing coefficients for polyimide repeat units

Dianhydride	Method	V_{mole}	α_{ZZ}	α_{XX}	α_{YY}	$\alpha_{av}/V_{molecule}$	$\Delta\alpha/V_{molecule}$	K_p
D2192-BAPP	STO 3G	529.74	516.59	306.01	250.14	0.1662	0.1108	0.5034
	6-31G	558.37	707.09	380.71	472.43	0.2293	0.1237	0.3648
6FDA-BAPP	STO 3G	530.55	401.39	375.21	279.46	0.1633	0.0214	0.4998
	6-31G	499.08	569.07	544.41	415.58	0.2514	0.0273	0.3247

STO 3G and 6-31G are two calculation methods in Gaussian 98W. V_{mole} is the mole volume of polyimides calculated by Gaussian 98W. α_{ZZ}, α_{XX}, and α_{YY} are the components of polarizability tensor for PI repeat unit in molecular frame where Z-axis is parallel to the PI main chain. $\alpha_{av}/V_{molecule}$, $\Delta\alpha/V_{molecule}$, and K_p are the average polarizability per volume, polarizability anisotropy per volume and estimated packing coefficient of polyimides, respectively.

Table 2
In-plane refractive indices (n_{TE}), out-of-plane refractive indices (n_{TM}), average refractive indices (n_{av}), in-plane/out-of-plane birefringence (Δn), and estimated intrinsic birefringence (Δn^0) of polyimides

Dianhydride	Method	n_{TE}	n_{TM}	n_{av}	Δn	Δn^0
D2192-BAPP	STO 3G	1.6179	1.6172	1.6177	0.0007	0.3240
	6-31G	–	–	–	–	0.2632
6FDA-BAPP	STO 3G	1.5996	1.5984	1.5992	0.0012	0.1014
	6-31G	–	–	–	–	0.0844

$n_{av} = [(2n_{TE}^2 + n_{TM}^2)/3]^{1/2}$, $\Delta n^0 = n_{||}^0 - n_{\perp}^0$.

PI films were also calculated based on the equations listed in Fig. 7.

We initially supposed that the higher induced birefringence at the same elongation can be attributed to the PI structure of higher Δn^0. Dr. Ando reported that the estimated values of Δn^0 for aromatic PIs correlates strong with $\Delta\alpha/V_{vdw}$. The same correlation was observed in our work with fluorinated PI and aliphatic PI. The replacement of V_{vdw} by $V_{molecule}$ had little effect on correlation. However, the estimated Δn^0 of 6F-B PI was found to be lower than that of D-B PI. This result implies that the stretch-induced birefringence may be more related to the chain–chain interaction rather than the ideal static-state of chain alignment.

In fact, 6F-B PI, because of its aromatic structure, had higher $\alpha_{av}/V_{molecule}$ than D-B PI. Although we have not stretched the PI films long enough to observe the full effect of intrinsic birefringence on the stretch-induced birefringence, the values of average polarizability per volume may strongly affect the value of the stretch-induced birefringence at a low-degree of elongation (0–40%). The higher $\alpha_{av}/V_{molecule}$ is, the stronger chain–chain interaction will be. The simulation work gave a reasonable explanation why 6F-B film showed a three-times larger birefringence than D-B film had after a low degree of stretching. It also predicts that the difference of induced birefringence between 6F-B film and D-B film may decrease or inverse at a high elongation ratio because of the higher calculated intrinsic birefringence of D-B PI. Moreover, the more intense relaxation of stretched 6F-B film at temperatures above T_g may be explained by its estimated packing coefficient that is lower than D-B PI. It also can be inferred that the higher chain–chain interaction in 6F-B film during the same stretching period might store a higher stress. The stress was then released at a temperature above T_g.

Calculations of polarizability tensor and intrinsic birefringence of the PI repeat unit truly give us much information to uncover the mystery of stretching-induced birefringence. Although in this work, we have simplified some of the procedures suggested in earlier work [12], further efforts will be focused on the calculation of higher-level theory with a better computer system. The elongation of PI films will also be prolonged to observe the full effect of intrinsic birefringence. Because of the significant effect of PI structure on the induced birefringence of stretched PI films, we can easily modify the compensation performance [9] of the PI films through designing the PI structure and controlling stretch condition. Nevertheless, we need to trade-off among many properties, such as transparence versus high dipole structures.

4. Conclusion

The stretch of PI films was successfully performed at 260 °C with our low-T_g polyimides. The D2192-BAPP film that shows high transparency to visible light is very suitable for many optical film applications, such as retardation films. The variations of in-plane and out-of plane birefringence during the stretching process were highly affected by PI structure. The packing coefficients (K_p) and the intrinsic birefringence (Δn^0) of aliphatic and aromatic polyimides were estimated using the experimentally obtained refractive indices (n_{av}) and the computationally calculated polarizability tensors (α_{XX}, α_{YY}, and α_{ZZ}). It was found that the intrinsic birefringence is not the dominant factor controlling the stretched-induced birefringence. The higher birefringence of 6F-B film in a low elongation range (0–40%) may be attributed to the higher average polarizability per volume ($\alpha_{av}/V_{molecule}$) from its aromatic structure. The lower K_p and the higher chain–chain interaction together cause the stretched 6F-B film to show more intense relaxation than the stretched D-B film did. Thus, the simulation work has given us a lot of information to uncover the mystery of stretching-induced birefringence. However, there is still a need to use a higher-level theory, such as B3LYP/6-31+G(d), to obtain a more accurate comparison. Moreover, the full effect of intrinsic birefringence on highly stretched PI films should be studied further.

References

[1] H. Ma, A.K.Y. Jen, L.R. Dalton, Adv. Mater. 14 (2002) 1339.
[2] M. Zhou, Opt. Eng. 41 (2002) 1631.
[3] S.Z.D. Cheng, F. Li, E.P. Savitski, F.W. Harris, Trip 5 (1997) 51.
[4] F. Li, F.W. Harris, S.Z.D. Cheng, Polymer 37 (1996) 5321.
[5] J. Chen, K.H. Jyu, J.J. Souk, J.H. Kelly, J.R.P.J. Bos, SID98 Dig. (1998) 315.
[6] Y. Saitoh, S. Kimura, K. Kusafuka, H. Shimizu, Jpn. J. Appl. Phys. 37 (1998) 4822.
[7] S.T. Wu, C.S. Wu, Liq. Cryst. 24 (1998) 811.
[8] I.M. Ward, Structure and Properties of Oriented Polymers, Applied Science Publishers, UK, 1975.
[9] J.S. King, W.T. Whang, W.C. Lee, L.M. Chang, Jpn. J. Appl. Phys. 45 (2006) L501.
[10] Y. Terui, S. Ando, J. Polym. Sci.: Polym. Phys. 42 (2004) 2354.
[11] S. Matsuda, S. Ando, J. Polym. Sci.: Polym. Phys. 41 (2003) 418.
[12] C.Y. Cha, R.J. Samuels, Proc. Soc. Plast. Eng. Annu. Tech. Conf. 39 (1993) 2896.
[13] P.K. Tien, Appl. Opt. 10 (1971) 2395.
[14] W.M. Prest Jr., D.J. Luca, J. Appl. Phys. 50 (1979) 6067.
[15] T. Takasaki, Y. Kuwana, T. Takahashi, S. Hayashida, J. Polym. Sci. A: Polym. Chem. 38 (2000) 4832.
[16] M. Hasegawa, K. Okuda, M. Horimoto, Y. Shindo, R. Yokota, M. Kochi, Macromolecules 30 (1997) 5745.